# Synthesis and Characterization of the Amphoteric Amino Acid Bifunctional Mesoporous Silica

Lu Han,[†] Juanfang Ruan,[‡] Yongsheng Li,[†] Osamu Terasaki,[‡] and Shunai Che*[,†]

*School of Chemistry and Chemical Technology, State Key Laboratory of Composite Materials, Shanghai Jiao Tong University, Shanghai 200240, P. R. China, Structural Chemistry, and Arrhenius Laboratory, Stockholm University, S-10691 Stockholm, Sweden*

*Received March 1, 2007. Revised Manuscript Received March 23, 2007*

New amphoteric, amino acid bifunctional mesoporous silicas with highly ordered mesopores were synthesized via the cooperative self-assembly of surfactants, co-structure-directing agents (CSDA), and a silica source. Uniform distributions of acid and base organic groups on the mesopore surfaces were formed by interactions between the counter charged surfactant head groups and ionic parts of CSDAs, that is, between the cationic and anionic surfactant head groups and the carboxyl and amino groups of CSDAs, respectively. For structural determination, the materials were characterized using X-ray diffraction (XRD), high-resolution transmission electron microscopy (HRTEM), and $N_2$ sorption measurements. It has been demonstrated that organic ($NH_2$ and COOH) pairs incorporated in the mesopore walls behave as amino acids, collectively exhibiting an isoelectric point, p*I*, of ∼6.0, a value close to that of a neutral amino acid. Further, the amphoteric amino acid moiety can be switched readily in a moment from net cationic and acidic to net anionic and basic by simply increasing the pH of the solution. Loading of the $NH_2$ and COOH groups was controlled at an almost equal basis of ca. 1.0 and 0.9 mmol/g $SiO_2$, respectively. Close adjacency of organic $NH_2$ and COOH groups was confirmed by the formation of amide moieties. The basic idea employed here will be easily and widely applicable to the design of relevant mesoporous materials.

## Introduction

Many research efforts have focused on synthesis of hybrid organic and inorganic mesoporous materials with functionalization of the exterior and/or interior surfaces aiming for applications in separation, adsorption, catalysis, sensor design, drug delivery, and nanotechnology.[1−12] Significant progress has been made in functionalization of many mesoporous silicas with various organic groups (alkyl,[13,14] vinyl/allyl,[15−17] amino,[17−22] thiol,[16,19] cyano,[17,23] alkoxy,[16] carboxyl,[20,24,25] aromatic,[13,16,23] organophosphine,[23] etc.) via postsynthesis grafting and organosiloxane/siloxane cocondensation. Two recent reports have dealt with the role of bifunctional, solid-support mesoporous materials as catalysts superior to the conventional monofunctionalized silica phases. Huh et al. have synthesized bifunctional mesoporous materials with ureidopropyl groups in cooperation with 3-[2-(2-aminoethylamino) ethylamino]-propyl groups to catalyze various reactions that involve carbonyl activation.[26] Zeidan et al. have functionalized the SBA-15 with sulfonic acid and amino groups; these have proven to be highly efficient catalysts in the aldol reaction as compared with materials carrying only one of the two functions.[27]

* To whom correspondence should be addressed. Fax: 86-21-5474-1297. Tel: 86-21-5474-2852. E-mail: chesa@sjtu.edu.cn.
[†] Shanghai Jiao Tong University.
[‡] Stockholm University.

(1) Dai, S.; Burleigh, M. C.; Shin, Y.; Morrow, C. C.; Barnes, C. E.; Xue, Z. *Angew. Chem., Int. Ed.* **1999**, *38*, 1235.
(2) Lin, V. S. -Y.; Lai, C.-Y.; Huang, J.; Song, S. -A.; Xu, S. *J. Am. Chem. Soc.* **2001**, *123*, 11510.
(3) Yoshitake, H.; Yokoi, T.; Tatsumi, T. *Chem. Mater.* **2003**, *15*, 1713.
(4) Qiao, S. Z.; Yu, C. Z.; Xing, W.; Hu, Q. H.; Djojoputro, H.; Lu, G. Q. *Chem. Mater.* **2005**, *17*, 6172.
(5) Rodriguez, I.; Iborra, S.; Corma, A.; Rey, F.; Jordá, J. L. *Chem. Commun.* **1999**, 593.
(6) Crudden, C. M.; Sateesh, M.; Lewis, R. *J. Am. Chem. Soc.* **2005**, *127*, 10045.
(7) Zhou, W.; Thomas, J. M.; Shephard, D. S.; Johnson, B. F. G.; Ozkaya, D.; Maschmeyer, T.; Bell, R. G.; Ge, Q. *Science* **1998**, *280*, 705.
(8) Basallote, M. G.; Blanco, E.; Blazquez, M.; Fernandez-Trujillo, M. J.; Litran, R.; Manez, M. A.; Ramirez del Solar, M. *Chem. Mater.* **2003**, *15*, 2025.
(9) Song, S. -W.; Hidajat, K.; Kawi, S. *Langmuir* **2005**, *21*, 9568.
(10) Yang, Q.; Wang, S.; Fan, P.; Wang, L.; Di, Y.; Lin, K.; Xiao, F. -S. *Chem. Mater.* **2005**, *17*, 5999.
(11) Ying, J. Y.; Mehnert, C. P.; Wong, M. S. *Angew. Chem., Int. Ed.* **1999**, *38*, 56.
(12) Raman, N. K.; Anderson, M. T.; Brinker, C. J. *Chem. Mater.* **1996**, *8*, 1682.
(13) Burkett, S. L.; Sims, S. D.; Mann, S. *Chem. Commun.* **1996**, 1367.
(14) Mercier, L.; Pinnavaia, T. J. *Chem. Mater.* **2000**, *12*, 188.
(15) Antochshuk, V.; Jaroniec, M. *Chem. Commun.* **2002**, 258.
(16) Fowler, C. E.; Burkett, S. L.; Mann, S. *Chem. Commun.* **1997**, 1769.
(17) Huh, S.; Wiench, J. W.; Yoo, J.-C.; Pruski, M.; Lin, V. S.-Y. *Chem. Mater.* **2003**, *15*, 4247.
(18) Che, S.; Garcia-Bennett, A. E.; Yokoi, T.; Sakamoto, K.; Kunieda, H.; Terasaki, O.; Tatsumi, T. T. *Nature Mater.* **2003**, *2*, 801.
(19) Walcarius, A.; Etienne, M.; Lebeau, B. *Chem. Mater.* **2003**, *15*, 2161.
(20) Lei, C.; Shin, Y.; Liu, J.; Ackerman, E. J. *J. Am. Chem. Soc.* **2002**, *124*, 11242.
(21) Gao, C.; Sakamoto, Y.; Sakamoto, K.; Terasaki, O.; Che, S. *Angew. Chem., Int. Ed.* **2006**, *45*, 4295.
(22) Gao, C.; Qiu, H.; Zeng, W.; Sakamoto, Y.; Terasaki, O.; Sakamoto, K.; Chen, Q.; Che, S. *Chem. Mater.* **2006**, *18*, 3904.
(23) Cagnol, F.; Grosso, D.; Sanchez, C. *Chem. Commun.* **2004**, 1742.
(24) Yang, C.-M.; Zibrowius, B.; Schüth, F. *Chem. Commun.* **2003**, 1772.
(25) Han, L.; Sakamoto, Y.; Terasaki, O.; Li, Y.; Che, S. *J. Mater. Chem.* **2007**, 17, 1216.
(26) Huh, S.; Chen, H.-T.; Wiench, J. W.; Pruski, M.; Lin, V. S.-Y. *Angew. Chem., Int. Ed.* **2005**, *44*, 1826.
(27) Zeidan, R. K.; Hwang, S.-J.; Davis, M. E. *Angew. Chem., Int. Ed.* **2006**, *45*, 6332.

10.1021/cm0705845 CCC: $37.00 
Published on Web 05/02/2007

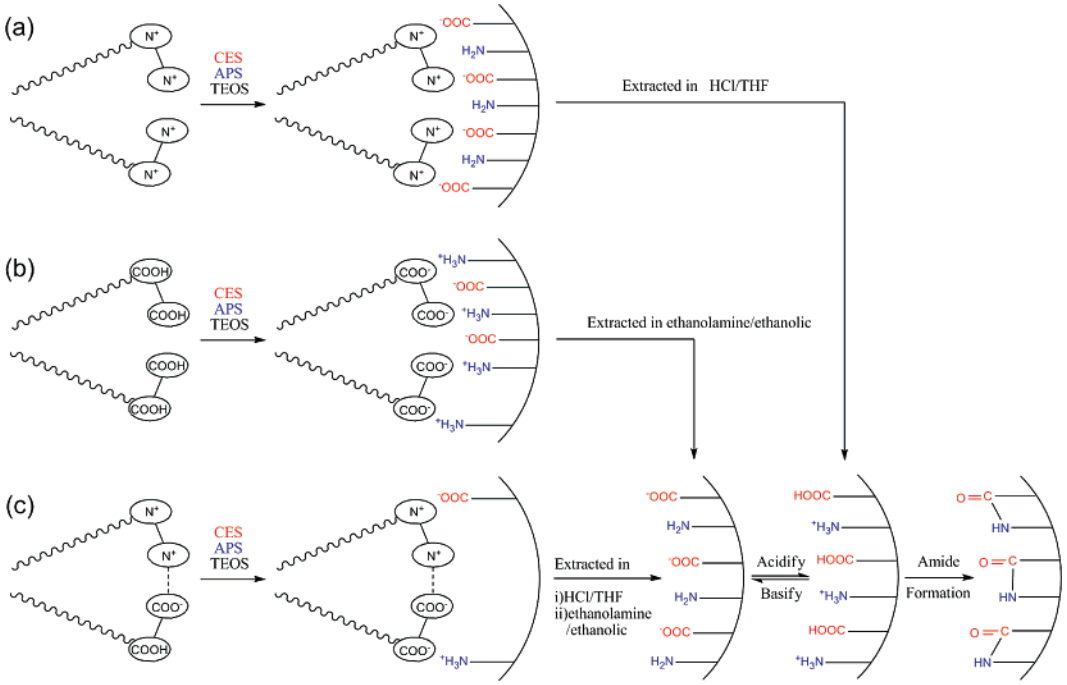


**Figure 1.** Schematic illustration of the interactions between the surfactant and the CSDAs (APS and CES) and switching process between the base and acid.

An amino acid, which contain both the carboxyl and amino groups as important moieties, is one of the essential biomolecules and is of central importance in biochemistry and pharmacology. There is a great interest in techniques for immobilizing amino acids on the surface of porous materials. Herein, we report a new, simple, and efficient synthetic approach for obtaining amphoteric mesoporous silica containing the symmetrical carboxyl group as a general acid and amino group as a general base, which would provide two-point attachments for biomolecules in a wide pH value range because of the $pK_a = 1-5$ of the carboxylic acid moiety and the $pK_b = 3.4$ of amino group. The amino acid functionality can vary from the cationic amino−carboxylic acid form to the zwitterionic form and then to the anionic amino−carboxylate form on changing from low to high pH. This amphoteric property makes mesoporous silica more valuable in, for example, biosensor, catalyst, and separation media, where both shape selectivity and enantioselectivity can be applied to the manufacturing of biochemicals and pharmaceuticals.

The synthesis of the bifunctional materials here is based on the co-structure-directing method proposed by Che et al.,[18,21,22,25] which can make the synthesis simple and efficient in producing a uniform distribution of the organic groups by the interaction between the surfactant (anionic surfactant or the cationic surfactant) and the CSDA (the organosilane, positively or negatively charged). It is worth noting that we have proven that the alteration of the charge density of the CSDA is an effective strategy for controlling the mesophase structure. We have succeeded in synthesizing the bifunctional mesoporous materials by three routes, using a cationic surfactant, an anionic surfactant, or the mixture of cationic and anionic surfactants. The amphoteric amino acid moiety can switch the ionic state in a moment from net cationic and acidic to net anionic and basic by simply increasing the solution pH.

## Experimental Section

**Chemicals.** All materials, tetraethyl orthosilicate (TEOS; SCRC, China), *N*,*N*-dimethyl-*n*-tetradecylamine (TCI, Japan), (3-bromopropyl)trimethylammonium bromide (Aldrich, USA), carboxyethylsilanetriol sodium salt (CES; Gelest, UK), 3-aminopropyltrimethoxysilane (APS; TCI, Japan), dicyclohexyl carbodiimide (DCC; SCRC, China), and triethylamine (SCRC, China), were used as purchased without further purification. Anionic surfactants derived from amino acids (glutamic acid, alanine, valine, etc.) were synthesized.

**Surfactant Preparation.** The gemini surfactant $[C_{18}H_{37}N(CH_3)_2(CH_2)_3N(CH_3)_3]Br_2$ ($C_{18-3-1}$) was synthesized according to ref 25. The anionic surfactant *N*-myristoyl-L-glutamic acid ($C_{14}$GluA) and *N*-stearoyl-L-glutamic acid ($C_{18}$GluA) were synthesized as described previously.[21,22] $C_{14}$GluA is used as the anionic surfactant for the mixed-surfactant synthesis. Therefore, one of the carboxyl groups of $C_{14}$GluA was neutralized by an equivalent molar amount of KOH to form *N*-myristoyl-L-glutamic acid-potassium salt ($C_{14}$GluAP), which will be active with $NH_2$ group of the CSDA (in this case, APS), and another carboxyl group was kept for the function of anionic surfactant.

**Synthesis of Mesoporous Silica.** The bifunctional mesoporous silicas were synthesized using cationic gemini surfactant $C_{18-3-1}$, the anionic surfactant $C_{18}$GluA, or the mixture of $C_{18-3-1}$ and $C_{14}$-GluAP, the mixture of APS and CES as CSDAs, and TEOS as the silica source.

Three different synthesis approaches were taken, as schematically shown in Figure 1.

*(I) Cationic Surfactant Templating Route.* In a typical synthesis of cationic surfactant-templated mesoporous materials, surfactant was dissolved in deionized water at room temperature, and CES, APS, and TEOS were then simultaneously added and the mixture was stirred for 2 h. The resultant solution was transferred to a Teflon bottle and heated at 100 °C for 2 days. Finally, the products were filtered and dried overnight under a vacuum at room temperature. The cationic surfactant was removed by refluxing 0.5 g of as-synthesized material in 100 mL of tetrahydrofuran (THF) with 1 M HCl solution for 12 h.

*(II) Anionic Surfactant Templating Route.* In the case of the anionic surfactant-templating system, $C_{18}$GluA was dissolved in deionized water at 80 °C. After the surfactant solution was cooled to 60 °C, the mixture of CES, APS, and TEOS was added with stirring. After 10 min, the stirring was stopped, and the reaction mixture was aged at 60 °C for 2 days. The precipitate was filtered and dried overnight under a vacuum at room temperature. The as-made sample was extracted with an ethanolic solution of ethanolamine (17 vol %) for 12−24 h at its boiling temperature.

*(III) Mixture of Cationic and Anionic Surfactant Templating Route.* The synthesis of the mixed-surfactant-templated bifunctional material is similar to the cationic surfactant-templating route. $C_{18-3-1}$ and $C_{14}$GluAP were dissolved in deionized water at 80 °C. After the surfactant solution was cooled to room temperature, the mixture of CES, APS, and TEOS was added simultaneously and then stirred for 2 h. The mixture was then transferred to a Teflon bottle and heated at 100 °C for 2 days. To obtain surfactant-free mesoporous silica functionalized with amino and carboxyl groups, we treated the as-made sample in the HCl/THF solution at first to remove the cationic surfactant, and then in ethanolamine/ethanolic solution to remove the anionic surfactant, for 12−24 h at their boiling temperatures.

In the acid−base switch process, the acid form or base form bifunctional material was suspended in an excess of 20% $NH_2C_2H_4$-$OH-H_2O$ (v/v) (or alkyl amine, e.g., ethylamine, propylamine) solution or 1 M $HCl-H_2O$ (or $H_2SO_4-H_2O$) solution for the basification or the acidification process, respectively. After the mixture was stirred at room temperature for 1 min, the material was completely basified or acidified. Then the resulting base form or acid form sample was filtered and dried overnight under a vacuum at room temperature. The switching process from acid to base and then from base to acid can be repeated several times.

**Peptide Coupling Reaction.** In a typical peptide coupling reaction, 0.1 g of acid form bifunctional material was suspended in 20 mL of dichloromethlane, and 0.15 mmol DCC and 0.25 mmol triethylamine were then added with stirring at room temperature. After 12 h, the product was separated by filtration and dried overnight under a vacuum at room temperature. The formation of amide was confirmed by (i) treating the sample with 1 M HCl at room temperature to confirm whether the sample was basified by triethylamine, and (ii) refluxing the sample in 35% HCl at 100 °C for hydrolysis of amide.

**Characterization.** Powder XRD patterns were recorded on a Rigaku X-ray diffractometer D/MAX-2200/PC equipped with Cu Kα radiation (40 kV, 20 mA) at the rate of 0.1°/min over the range of 1−6° ($2\theta$). HRTEM observations were performed with a JEOL JEM-3010 microscope operating at 300 kV (Cs = 0.6 mm, resolution 1.7 nm). Images were recorded with Kodak electron film SO-163 using low-electron-dose conditions. Fourier transform infrared (FTIR) spectra were recorded on Perkin-Elmer Paragon 1000 spectrometer with a resolution of 2 $cm^{-1}$ using the KBr method. The nitrogen adsorption−desorption isotherms were measured at 77 K with Quantachrome Nova 4200E. $^{13}C$ CP/MAS NMR spectra were measured on a MERCURYplus 400 spectrometer at 100 MHz and a sample spinning frequency of 3 kHz. The elemental analysis of the materials was obtained from a Perkin-Elmer Series II CHNS/O Analyzer 2400.

## Results and Discussion

**1. Synthesis Strategy.** The formation of amino acid bifunctional mesoporous silica is based on self-assembly in the system of surfactant, CSDA (APS or CES), and TEOS. For the surfactant, we can choose three different cases, (i) cationic, (ii) anionic, or (iii) a mixture of cationic and anionic surfactants. Mesoporous materials hardly form without APS or TMAPS in the anionic surfactant templating system.[18,21,22] Here, we have also found that the mixture of anionic and cationic surfactants could not produce well-ordered mesoporous materials without a CSDA. Although the alteration of the structure of the micelle has been an effective strategy for controlling the mesophase structure, we have proven that the CSDA produces a dominating effect on the type of mesostructures prepared under different synthesis conditions by controlling the charge density due to the charge matching between the surfactant and CSDA.[21,22] In the cationic surfactant synthesis system, ordered mesostructures can be formed without CES; however, we found CES still played an important role on the formation of the mesoporous materias.[25] We defined CSDA from the viewpoint of the indispensability and dominating effect of CSDA for the formation of mesostructure.

Figure 1a−c shows the synthesis pathways using the cationic surfactant, anionic surfactant, and the mixture of cationic and anionic surfactants, respectively.

As shown in Figure 1a, in the cationic surfactant templating route, the gemini surfactant ($C_{18-3-1}$) was used. These surfactants self-assemble to form a micelle with quaternary ammonium groups on the surface. With the addition of APS, CES, and TEOS, the positively charged head group of $C_{18-3-1}$ interacts electrostatically with the negatively charged carboxylate site of CES, through double decomposition of the cationic surfactant salt and the CES carboxylate salt. The triol site of CES was co-condensed with the silica source TEOS, and subsequently formed the silica network. The ethylene groups of CES covalently tether the silicon atoms incorporated in the framework to the anionic carboxylate groups. In the cationic surfactant-templating route (Figure 1a), the hydrophobic alkoxysilane part of APS can play a role in its uniform dispersion in the hydrophobic part of $C_{18-3-1}$ in the beginning of the reaction, which would be distributed on the pore surface uniformly during the synthesis via co-condensation with the silica source. After removal of the cationic surfactant by exhaustive solid−liquid extraction using HCl/THF, the carboxyl and protonated ammonium groups remain on the surface of the mesopores.

In the anionic surfactant-templating route (Figure 1b), $C_{18}$-GluA was used. These surfactants self-assemble to form a micelle with carboxyl groups on the surface. In a manner opposite to the cationic surfactant-templating route, the negatively charged head group of the anionic surfactant interacts with the positively charged ammonium site of APS through a neutralization reaction. The alkoxysilane sites of APS are co-condensed with TEOS to form the silica framework. However, in the anionic surfactant-templating route, the negatively charged carboxylate site of CES would repel itself from the negatively charged silica wall; it could not interact with any site in the micelle and would distort the micelle formation of $C_{18}$GluA, which leads to a nonuniform carboxylate distribution and disordered mesostructure. The as-made sample can be treated in ethanolamine/ethanolic solution to remove the surfactant, leaving the carboxylate and amino groups on the surface of the mesopores.

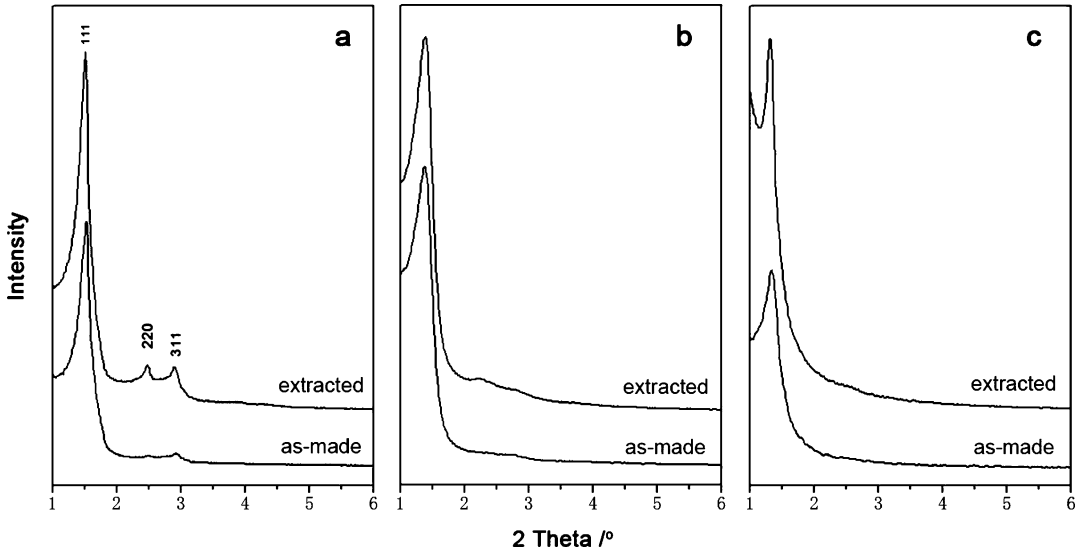


**Figure 2.** Powder XRD patterns of the as-made and extracted samples of (a) cationic surfactant-templated bifunctional material (the molar composition of the synthesis mixture was 1:1:1:15:2000 $C_{18-3-1}$:APS:CES:TEOS:$H_2O$); (b) anionic surfactant-templated bifunctional material (the molar composition was 1:2:2:2:15:2000 $C_{18}$GluA:APS:CES:HCl:TEOS:$H_2O$); (c) mixture surfactant-templated bifunctional material (the molar composition was 1:0.5:2:2:15:2000 $C_{18-3-1}$:$C_{14}$GluAP:APS:CES:TEOS:$H_2O$).

In Figure 1c, the mixture of the anionic surfactant $C_{14}$-GluAP (with one carboxyl and one carboxylate group) and cationic surfactant $C_{18-3-1}$ (with two quaternary ammonium groups) are shown. The negatively charged carboxylate group of $C_{14}$GluAP can electrostatically interact with the positive charge in the head group of $C_{18-3-1}$, leading to double decomposition of the carboxylate salt site of $C_{14}$GluAP's with the quaternary ammonium salt site of $C_{18-3-1}$, whereas the carboxyl group of the $C_{14}$GluAP and the other quaternary ammonium group of $C_{18-3-1}$ remain unreacted. Thus, the anionic surfactant and cationic surfactant self-assemble to form a micelle with both carboxyl and quaternary ammonium groups on the surface. When the mixture of the CSDAs is added to the solution of the mixed surfactants, the negatively charged carboxylate site of CES interacts with the positively charged quaternary ammonium head group of $C_{18-3-1}$ and the ammonium site of APS interacts with the negatively charged carboxyl group of $G_{14}$GluAP electrostatically and distribute stoichiometrically according to the arrangement of the surfactants. The triol site of CES and the alkoxysilane site of APS co-condensed with the silica source TEOS to form the silica network. It can be considered that proper APS/surfactant and CES/surfactant molar ratio could result in a pH of the system being favorable for the condensation of alkoxysilane. In this mixed-surfactant-templating route, the anionic surfactant and the cationic surfactant can be removed by a two-step extraction using HCl/THF and ethanolamine/ethanolic solutions, consecutively.

Obviously, (i) at high pH, carboxyl and protonated ammonium groups can release a proton and become carboxylate and amino groups, respectively, and (ii) at low pH, the carboxylate and amino groups can accept a proton and become carboxyl and protonated ammonium groups, respectively, via the zwitterionic state. Because of both the acid and base groups on the wall, the mesoporous silica thus formed can be amphoteric.

**2. Characterization of the Mesostructure.** The XRD pattern (Figure 2) of sample (a) synthesized using cationic surfactant shows a sharp peak in the region of $2\theta = 1.5-2.0°$ and two additional weak peaks in the region of $2\theta$ close to 2.6 and 3.2°. They are indexed to the 111, 220, and 311 reflections on the basis of the cubic crystal system, which will be confirmed later by HRTEM, with the unit-cell dimension $a = 90.7$ Å. Sample (b) synthesized by anionic surfactant shows an intense peak in the region of $2\theta = 1.0-1.5°$ and two additional weak peaks in the region of $2\theta$ close to 2.3 and 2.8°, which indicate the presence of mesostructure. The sample (c) obtained from the mixture surfactant displays a strong peak in the range $2\theta = 1.0-1.5°$, which suggests the formation of mesostructure in the prepared powder.

Three extracted mesoporous silicas in Figure 2 were further examined by TEM (Figure 3). The HRTEM images of sample (a) taken along the [110] and [211] directions are shown in $a_1$ and $a_2$ of Figure 3, respectively. The corresponding Fourier diffractograms (FDs) shown in the insets indicate extinction conditions for the reflections. The sample was tilted to obtain a series of electron diffraction (ED) patterns (Figure $3a_3$). From observations in the FDs and the systematic tilting series of ED patterns, observed reflections are summarized as the following conditions {*hkl*: $h + k =$ even, $k + l =$ even, $h + l =$ even; 0*kl*: $k, l =$ even; *hhl*: $h + l =$ even; 00*l*: $l =$ even}. The conditions suggested that the possible space groups of $F23$, $Fm\bar{3}$, $F432$, $F\bar{4}3m$, or $Fm\bar{3}m$, and we chose $Fm\bar{3}m$ because of the highest symmetry. The HRTEM image in Figure $3a_1$ shows that the extracted bifunctional material is a mixture of mostly the cubic close-packed $Fm\bar{3}m$ phase and a relatively small amount of the 3D hexagonal close-packed phase, which is commonly observed in $Fm\bar{3}m$ cubic silica mesoporous materials. The HRTEM image of sample (b) is shown in Figure 2b. These images provide evidence that the pore structures of the extracted sample (b) (using $C_{18}$GluA as structure-directing agent) exhibit a disordered cage-type mesostructure (with disorder in the mesopore shape). HRTEM image of sample (c) shown in Figure 3c suggested that

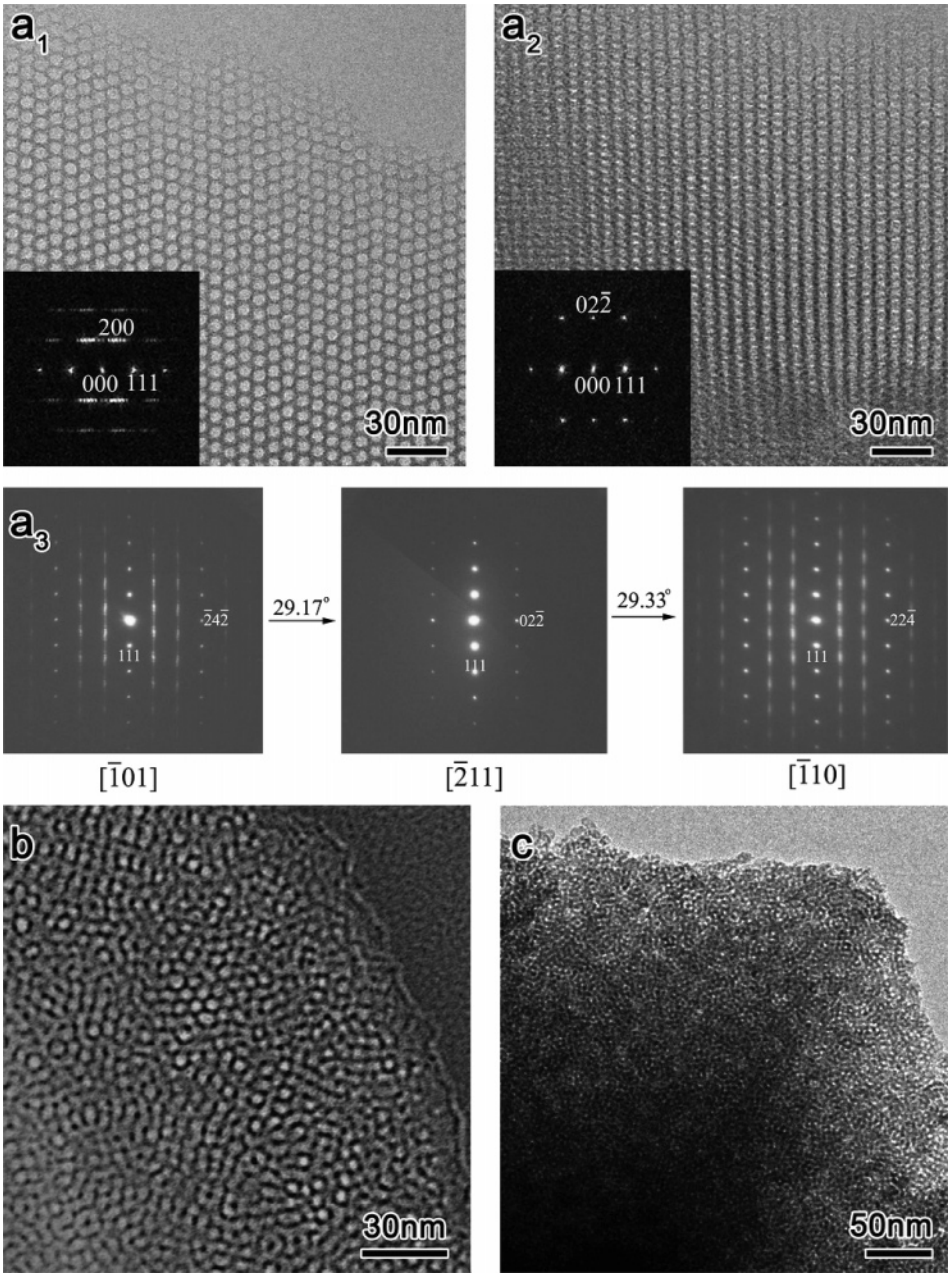


**Figure 3.** TEM images of the extracted bifunctional materials shown in Figure 2 ($a_1$, $a_2$, b, and c) and a series tilted selected-area electron diffraction patterns ($a_3$).

the sample (c) synthesized by the mixture of anionic and cationic surfactants has a disordered mesopore structure with a pore size of ca. 4 nm.

**3. Amphoteric Properties.** The results of XRD and TEM clearly show that the cationic surfactant-templated mesoporous silica has the best ordered structure. According to the best structure and the possibility of the uniform distribution of the organic groups, the cationic surfactant-templated mesoporous silica was chosen as the amphoteric amino acid bifunctional material for the characterization of amphoteric properties. The synthesis yield of the bifunctional material was ~86%. The existence of the functional groups and the removal of the surfactant were confirmed by the solid-state $^{13}C$ MAS NMR spectrum before and after extraction (Figure 4). The strong resonance peaks, assignable to $CH_2$ group of the surfactants, disappeared after extraction, indicating that the surfactants were completely extracted. In the $^{13}C$ MAS NMR spectrum of extracted sample, the resonance signals at 8.3, 20.5, and 41.8 ppm correspond to $C_I$, $C_{II}$, and $C_{III}$ of APS,[17,22] and those at 6.5, 26.2, and 176.5 ppm correspond to $C_{IV}$, $C_V$, and $C_{VI}$ of CES,[24,25] respectively. The other peaks reveal that both of the CES and APS are incorporated in the material.

Quantitative determination of the functional groups was carried out by CHN elemental chemical analysis. The loading level of $NH_2$, and the carbon content sourced from APS were calculated by the nitrogen content of the analytic result, and the loading level of COOH was calculated by the residual carbon content. The analytical results show that the loading amount of the $NH_2$ and COOH organic groups were ca. 1.0 and 0.9 mmol/g $SiO_2$, respectively, indicating that the amino and carboxyl groups were co-condensed with TEOS and introduces as initially loaded. The theoretical loading of both functional groups is 1.0 mmol/g $SiO_2$.

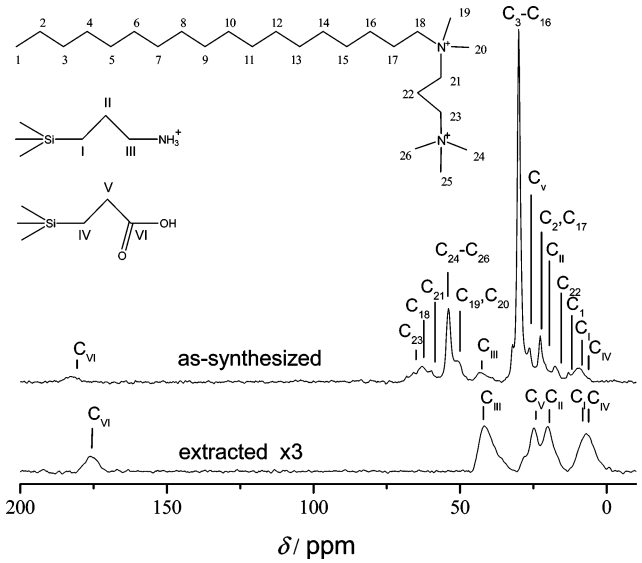


**Figure 4.** $^{13}C$ MAS NMR spectra of the as-synthesized and extracted sample shown in Figure 2a.

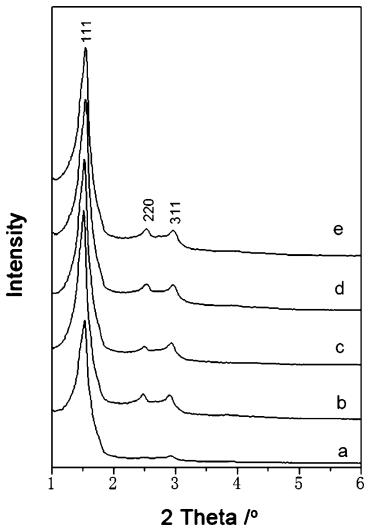


**Figure 5.** Powder XRD patterns of the (a) as-synthesized, (b) the initial extracted acid form, (c) the first switched base form, (d) the tenth switched acid form, and (e) the tenth switched base form amino acid bifunctional mesoporous silicas synthesized by cationic surfactant.

The bifunctional material behaves as an acid or base depending on the different conditions. After removing the surfactant, various $RNH_2$ and strong mineral acids with high concentrations could be used as basifying and acidifying agents to obtain the base and acid form amphoteric materials, respectively. As expected, the amphoteric acid−base switching occurred in several seconds, which has been tested more than 10 times. Figure 5 shows the powder XRD patterns of the as-synthesized, the first, and the tenth switched acid and base form bifunctional mesoporous silicas, respectively. All samples displayed an intense XRD peak in the region of $2\theta = 1.5-2.0°$ and two additional weak peaks in the region of $2\theta$ close to 2.6 and 3.2°. Judging from the intensity of the samples, it can be considered that the ordering of the pore arrangement was improved by the removal of the surfactant and retained even after the switching was repeated 20 times.

The $N_2$ adsorption−desorption analysis of the extracted bifunctional mesoporous silica revealed typical type IV isotherms (Figure 6). The measured BET (Brunauer−Emmett−Teller) surface area was 558.12 $m^2/g$. The corresponding BJH (Barrett−Joyner−Halenda) average pore diameter of the material was 3.78 nm and the pore volume was 0.48 $cm^3/g$. However, the pore volume and the surface area of the samples switched 20 times were slightly increased because of the thinner silica wall caused by hydrolysis during the basification process.

At first, the changes between carboxyl and carboxylate in the acid and base forms were confirmed by the FTIR spectrum of the switched samples (Figure 7). The band appearing at 1718 $cm^{-1}$ corresponding to the C═O stretching vibration demonstrates the existence of COOH in the acidic samples (plots b and d in Figure 7), which disappeared when the samples were switched to their base forms. The band corresponding to carboxylate would appear at 1560 $cm^{-1}$, which overlapped with the vibration of band N−H amino group.

Second, the change from the basic amino group to $NH_3^+Cl^-$ was confirmed by detecting the $Cl^-$ ion in an aqueous suspension of the mesoporous sample. The acidic samples with $NH_3^+Cl^-$ groups and the basic amino-bearing samples were dispersed separately in deionized water. After the samples were deposited on the bottom of the bottle and the solution became clear, silver nitrate solution was added to the aqueous solution. As expected, in the former, a white precipitate was produced that was due to the presence of $Cl^-$ from the $NH_3^+Cl^-$ group, whereas the latter solution remained clear (see the Supporting Information, Figure S1). In addition, no white precipitate was produced by adding $AgNO_3$ to the aqueous suspension of the calcined sample that was treated in HCl and washed. These observations are evidence that COOH and $NH_3^+$ groups could be simultaneously switched to $COO^-$ and $NH_2$ groups in the presence of strong alkali and reversely switched in the presence of strong acid.

**4. Isoelectric Point.** The isoelectric point of this amino acid bifunctional mesoporous silica has been obtained by measuring the pH changes upon titration of basic solution as shown in Figure 8. The isoelectric point of this material was estimated to be ∼6.0, which is similar to that of the neutral amino acid. The titration experiment gave COOH and $NH_2$ group loadings of 1.0 and 1.0 mmol/g of $SiO_2$, respectively, which coincide with the results of the elemental chemical analysis.

**5. Peptide Formation by Coupling Reaction.** The adjoining presence of amino-acid pairs has been confirmed by the formation of amide. It is reasonable that amide can be prepared from the carboxylic acid and the protonated ammonium groups neighboring each other on the pore surface in the presence of DCC as peptide coupling reagent under basic conditions. Figure 9 shows IR spectra of samples before and after amide formation. After the amide formation reaction, the band at 1718 $cm^{-1}$ (corresponding to C═O of COOH) disappeared without destruction of the mesostructure (see the Supporting Information, Figure S2). However, the band corresponding to carbonyl of the amide which appear at ∼1680 $cm^{-1}$ is indiscernible, largely because of the overlapping with the band at ∼1630 $cm^{-1}$ attributed to the vibration of adsorbed water and others from the frame

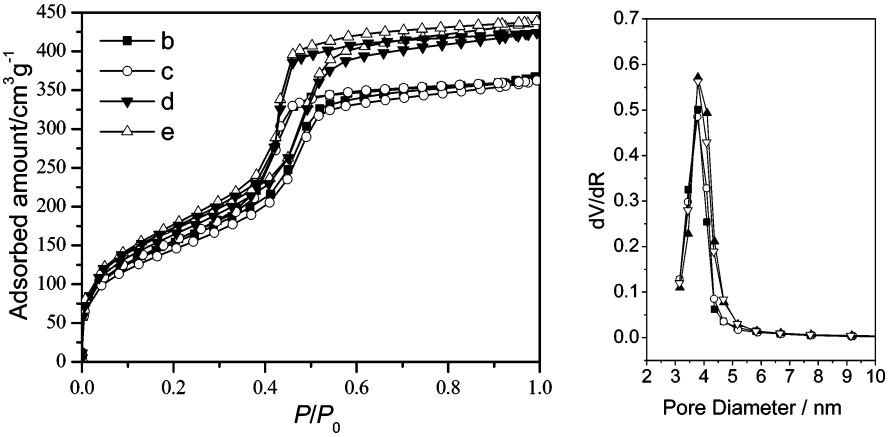


**Figure 6.** Nitrogen adsorption isotherms and corresponding pore size distribution curves of amino acid bifunctional mesoporous silicas in Figure 5.

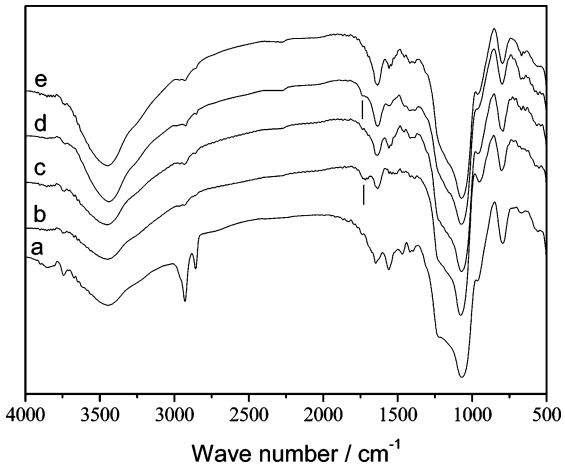


**Figure 7.** FTIR spectra of the amino acid bifunctional mesoporous silicas shown in Figure 5.

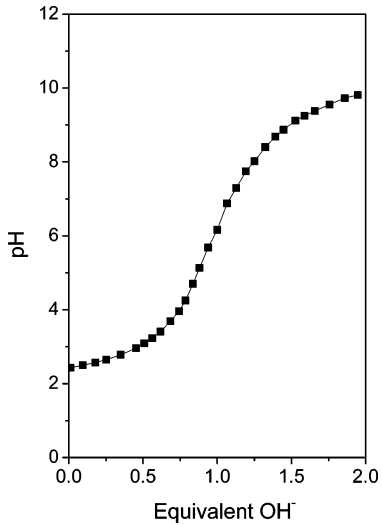


**Figure 8.** pH of the amino acid bifunctional mesoporous silica solution titrated with a strong base of NaOH.

symmetric and antisymmetric flexible vibration of Si groups.[28] However, an amide band was observed at 1568 cm$^{-1}$. From these observations, two reactions, i.e., the neutralization with triethylamine or the amide formation, may happen. Therefore amide formation has been confirmed by neutralization and hydrolysis. In contrast to the carboxylate neutralization

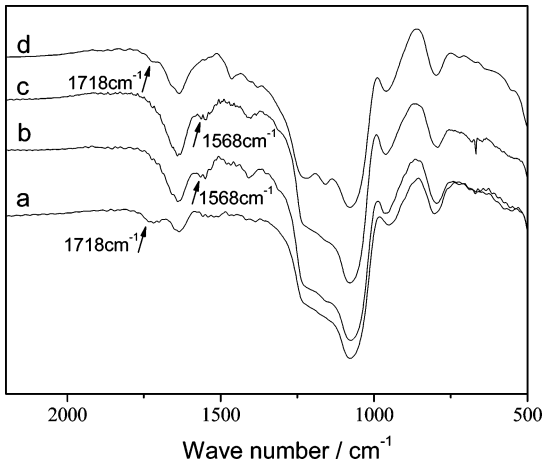


**Figure 9.** FTIR spectrum of (a) the extracted sample, (b) the DCC-promoted amide-containing material obtained by reacting the carboxylic acid with the protonated ammonium groups on the pore surface, (c) the amide-containing sample treated with 1 M HCl at room temperature for 4 h, and (d) that refluxed in 35% HCl at 100 °C for 4 h.

shown before (Figure 7), the amide sample did not show the band of COOH at 1718 cm$^{-1}$, even after reacting in 1 M HCl−$H_2O$ solution for several hours while the band at 1568 cm$^{-1}$ could still be observed. On the other hand, the COOH band at 1718 cm$^{-1}$ appeared in the hydrolyzed sample and the band at 1568 cm$^{-1}$ disappeared, indicating that such material can consist of uniformly distributed amino-acid pairs.

## Conclusion

To the best of our knowledge, this is the first synthesis of amphoteric bifunctional mesoporous silica with amino and carboxyl groups. The highly ordered mesoporous silica was synthesized with the simple cationic surfactant and the mesocages are arranged in cubic closed packing with $Fm\bar{3}m$ symmetry. We can easily introduce the amino and the carboxyl groups, which adjoin on the silica−mesopore wall, and it was confirmed that the groups showed the same function as amino acids when the pH of the solution was changed. In other words, a pseudo-amino acid was successfully formed and immobilized to the surface of the mesoporous wall. This new methodology for synthesizing multifunctionalized mesoporous materials may open a new channel to a wide variety of bioinspired functional materials.

(28) Anderson, M. W.; Klinowski, J. *J. Chem. Soc., Faraday Trans.* **1986**, *182*, 1449.

**Acknowledgment.** This work was supported by the National Natural Science Foundation of China (Grants 20425102, 20521140450, and 20501015) and the China Ministry of Education. O.T. thanks the Swedish Science Research Council (VR) and the Japan Science and Technology Agency (JST) for financial support. S.C. thanks Dr. Kazutami Sakamoto (Shiseido Co. Japan) and Prof. Yoshihisa Inoue (Osaka University, Japan) for scientific discussions. The authors are grateful to the Instrumental Analysis Center, Shanghai Jiao Tong University, for taking elemental analysis. The authors acknowledge Dr. Robert Corkery, YKI (Stockholm University) for his critical reading and comments.

**Supporting Information Available:** The XRD patterns of the DCC-promoted amide-containing material and pictures of aqueous suspension of the different samples. This material is available free of charge via the Internet at http://pubs.acs.org.

CM0705845